

SUPPLEMENTARY MATERIAL

Table of contents

Fig. S1. Decidual gene expression is not modulated by IL-1 α or aIL-6R

Fig. S2. Intra-amniotic IL-1 α , or treatment with aIL-6R, does not drastically modify neonatal ability to complete the neuromotor tests for surface righting and cliff aversion

Fig. S3. Neonatal gut microbiota composition is modified by intra-amniotic IL-1 α , which is partially rescued by aIL-6R treatment

Fig. S4. Blockade of IL-6R modifies the abundance of specific bacterial taxa in the neonatal caecum and colon

Fig. S5. Leukocyte proportions in the neonatal gut after intra-amniotic IL-1 α exposure or treatment with aIL-6R

Table S1. TaqMan assays utilised for RT-PCR

Table S2. List of antibodies utilised for flow cytometry

Table S3. Preterm labour-associated differential expression of *Il6* in murine uterine and decidual cell types

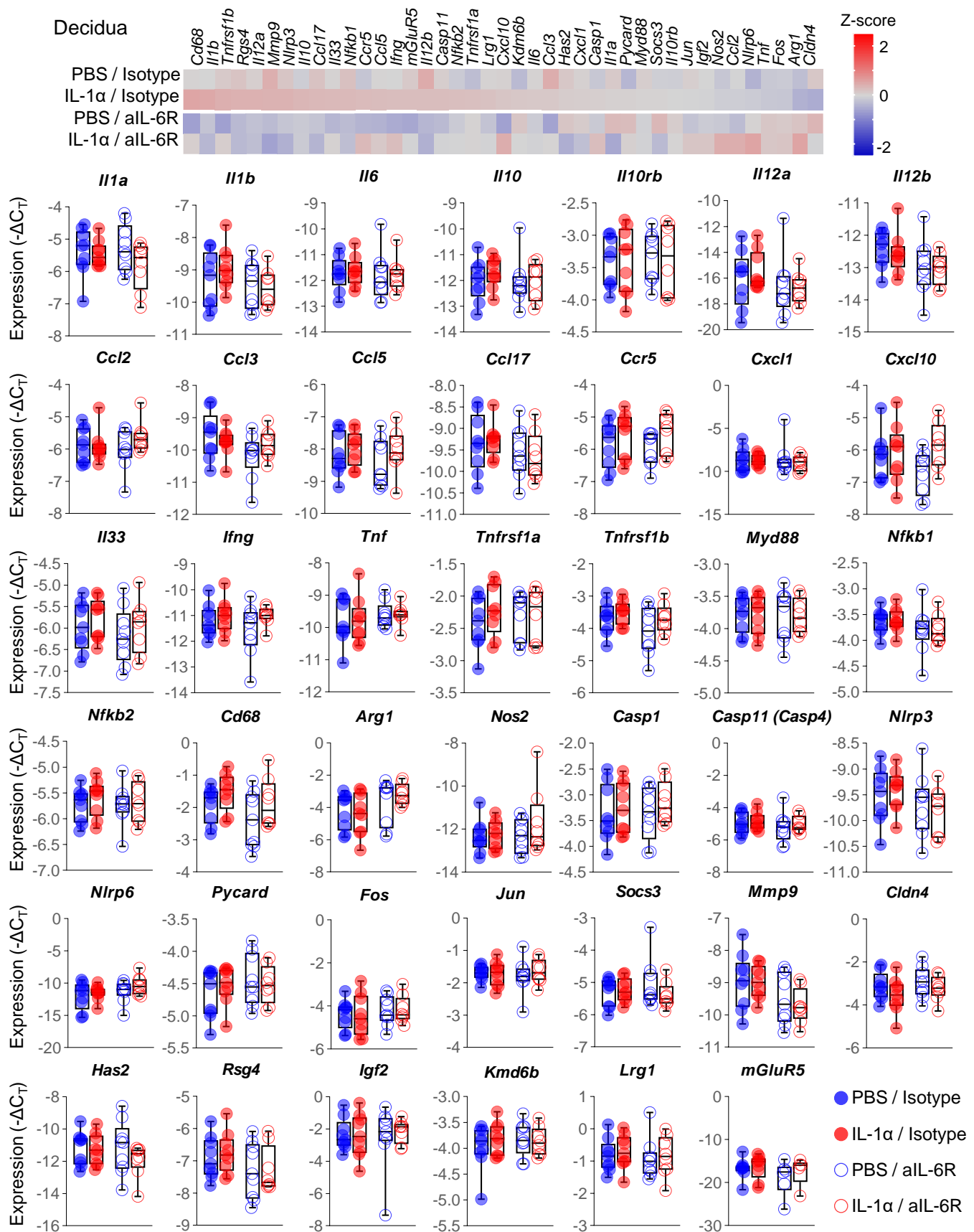


Fig. S1. Decidual gene expression is not modulated by IL-1 α or aIL-6R. Representative heatmaps showing Z-scores for gene expression in the decidua (n = 8-9 per group). Red indicates increased expression and blue indicates decreased expression. The expression ($-\Delta C_T$) of *Il1a*, *Il1b*, *Il6*, *Il10*, *Il10rb*, *Il12a*, *Il12b*, *Ccl2*, *Ccl3*, *Ccl5*, *Ccl17*, *Ccr5*, *Cxcl1*, *Cxcl10*, *Il33*, *Ifng*, *Tnf*, *Tnfrsf1a*, *Tnfrsf1b*, *Myd88*, *Nfkb1*, *Nfkb2*, *Cd68*, *Arg1*, *Nos2*, *Casp1*, *Casp11 (Casp4)*, *Nlrp3*, *Nlrp6*, *Pycard*, *Fos*, *Jun*, *Socs3*, *Mmp9*, *Cldn4*, *Has2*, *Rgs4*, *Igf2*, *Kdm6b*, *Lrg1*, and *mGluR5* is represented as box-and-whisker plots where midlines indicate medians, boxes indicate interquartile ranges, and whiskers indicate minimum and maximum values.

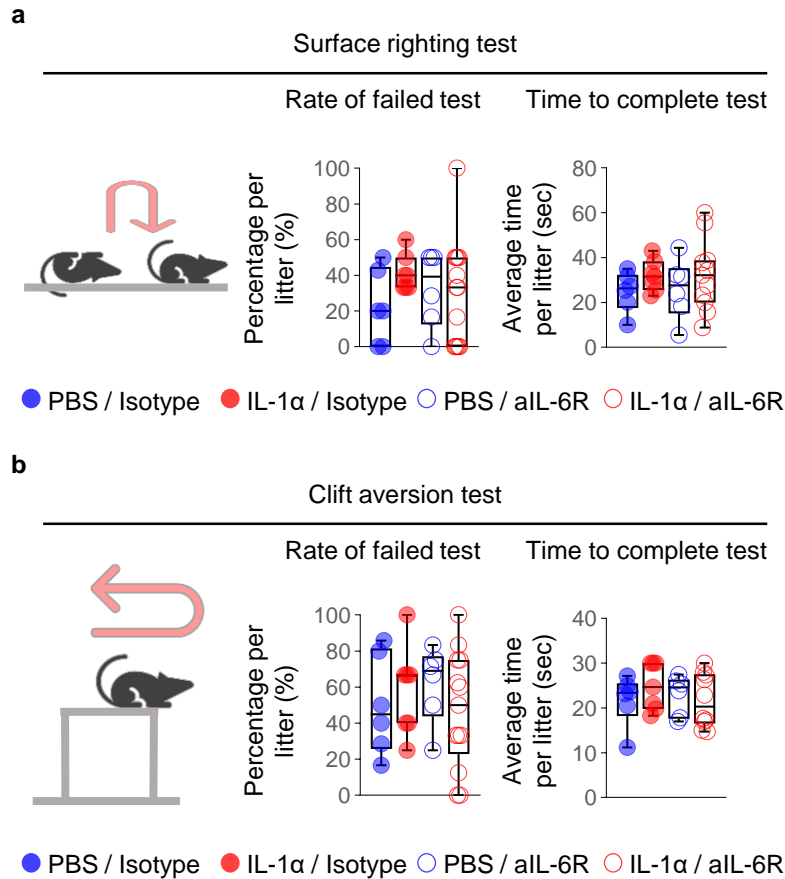


Fig. S2. Intra-amniotic IL-1 α , or treatment with aIL-6R, does not drastically modify neonatal ability to complete the neuromotor tests for surface righting and cliff aversion. (a) Schematic diagram of the surface righting test, and quantification of the rate of neonates with a failed test and the time required to complete the test (n = 6-14 litters per group). (b) Schematic diagram of the cliff aversion test, and quantification of the rate of neonates with a failed test and the time required to complete the test (n = 6-14 litters per group). Data are shown as box-and-whisker plots where midlines indicate medians, boxes indicate interquartile ranges, and whiskers indicate minimum and maximum values.

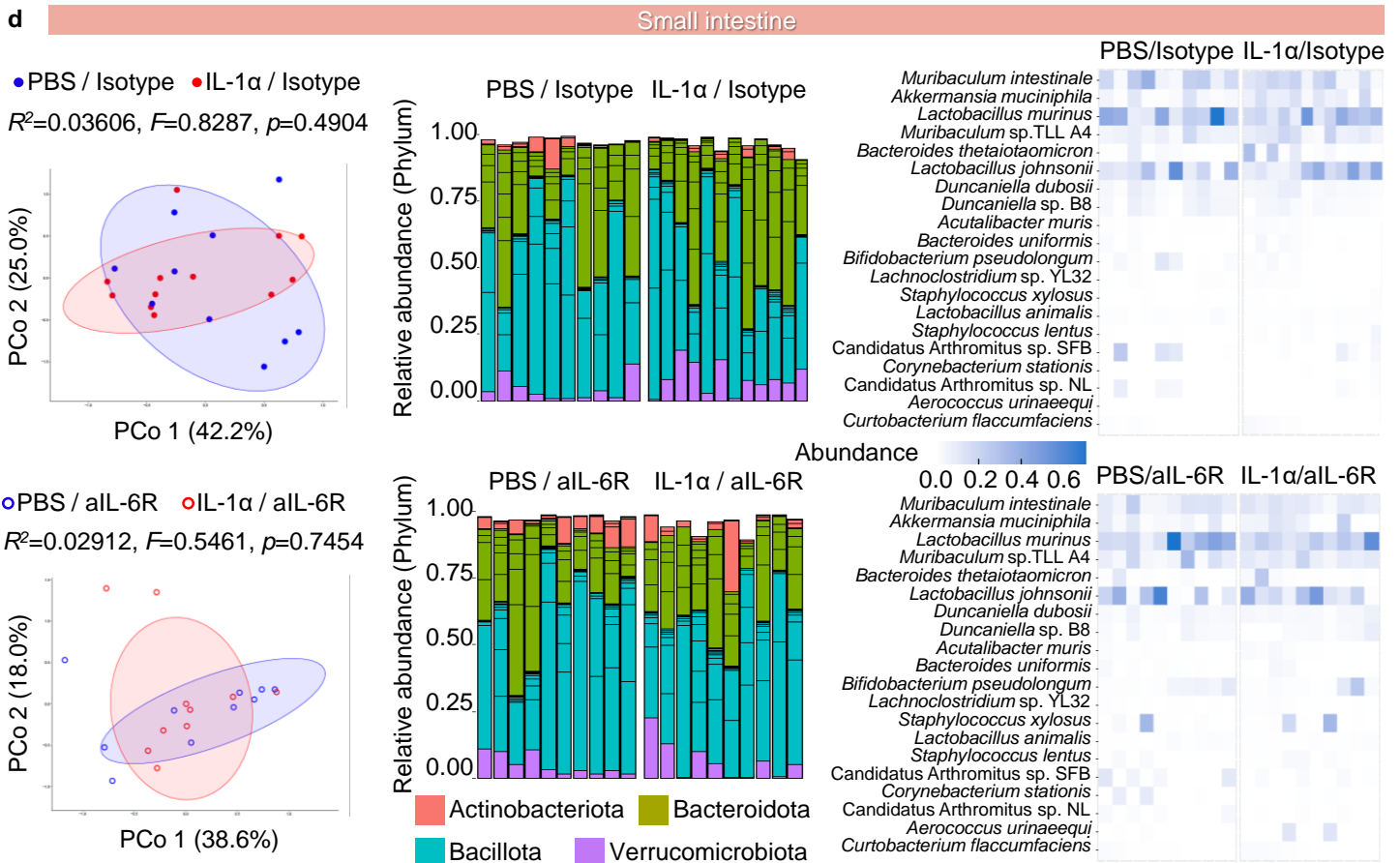
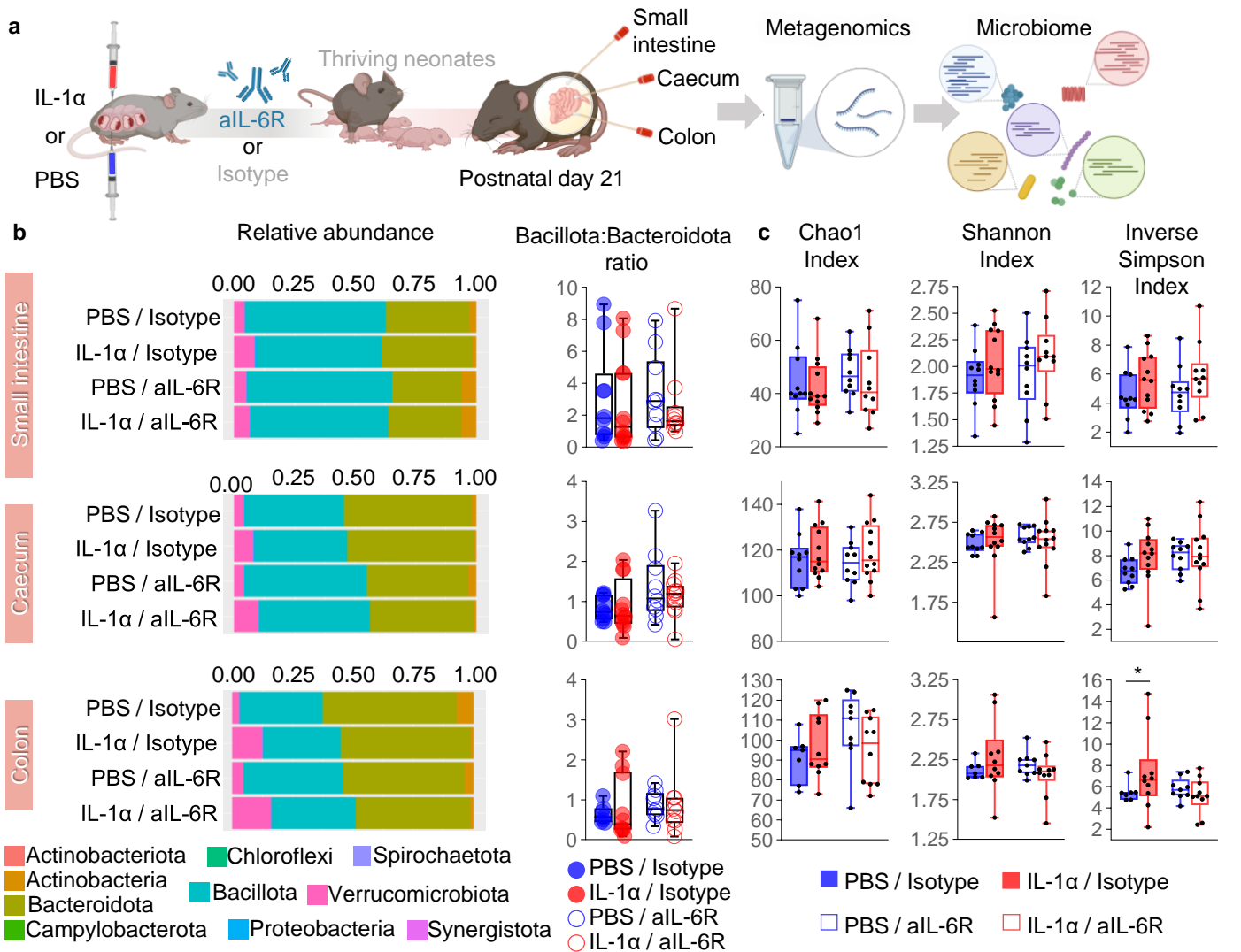


Fig. S3. Neonatal gut microbiota composition is modified by intra-amniotic IL-1 α , which is partially rescued by aIL-6R treatment. (a) Dams underwent intra-amniotic injection of PBS (control) or IL-1 α on 16.5 days post coitum (dpc). Six h later, dams received intraperitoneal injection of rat anti-mouse IL-6 receptor monoclonal antibody (aIL-6R) or rat IgG2b isotype (control). Dams were allowed to deliver, and the neonatal small intestine, caecum, and colon were collected on postnatal day (PDN) 21 for microbiome analysis using metagenomic sequencing. **(b)** Differences in abundance of major bacterial phyla (bar plots) and change in the Bacillota:Bacteroidota ratio in the neonatal small intestine, caecum, and colon are shown as box plots where midlines indicate medians, boxes indicate interquartile range, and whiskers indicate minimum/maximum range (n = 7-12 per group). **(c)** Alpha-diversity metrics for the microbiota composition of the neonatal small intestine, caecum, and colon from the four experimental groups (n = 7-12 per group). Data are shown as box-and-whisker plots where midlines indicate medians, boxes indicate interquartile ranges, and whiskers indicate minimum and maximum values. **(d)** Left: principal coordinate analysis (PCoA) illustrating variation in the metagenomic profiles of the neonatal small intestine of the PBS / Isotype and IL-1 α / Isotype groups or PBS / aIL-6R and IL-1 α / aIL-6R groups (n = 10-12 per group). Similarities in the metagenomic profiles (PCoA plots) were characterized using the Bray-Curtis similarity index. Middle: bar plots showing the taxonomic classifications of the 20 bacterial taxa with highest relative abundance in the neonatal intestine of the PBS / Isotype and IL-1 α / Isotype groups or PBS / aIL-6R and IL-1 α / aIL-6R groups (n = 10-12 per group). Right: heatmap displaying the relative abundance and taxonomy of the 20 most relatively abundant bacterial taxa between the metagenomic profiles of the neonatal intestine of the PBS / Isotype and IL-1 α / Isotype groups or PBS / aIL-6R and IL-1 α / aIL-6R groups (n = 10-12 per group). For heatmaps, bacterial taxa with significantly altered abundance between groups are labelled in blue.

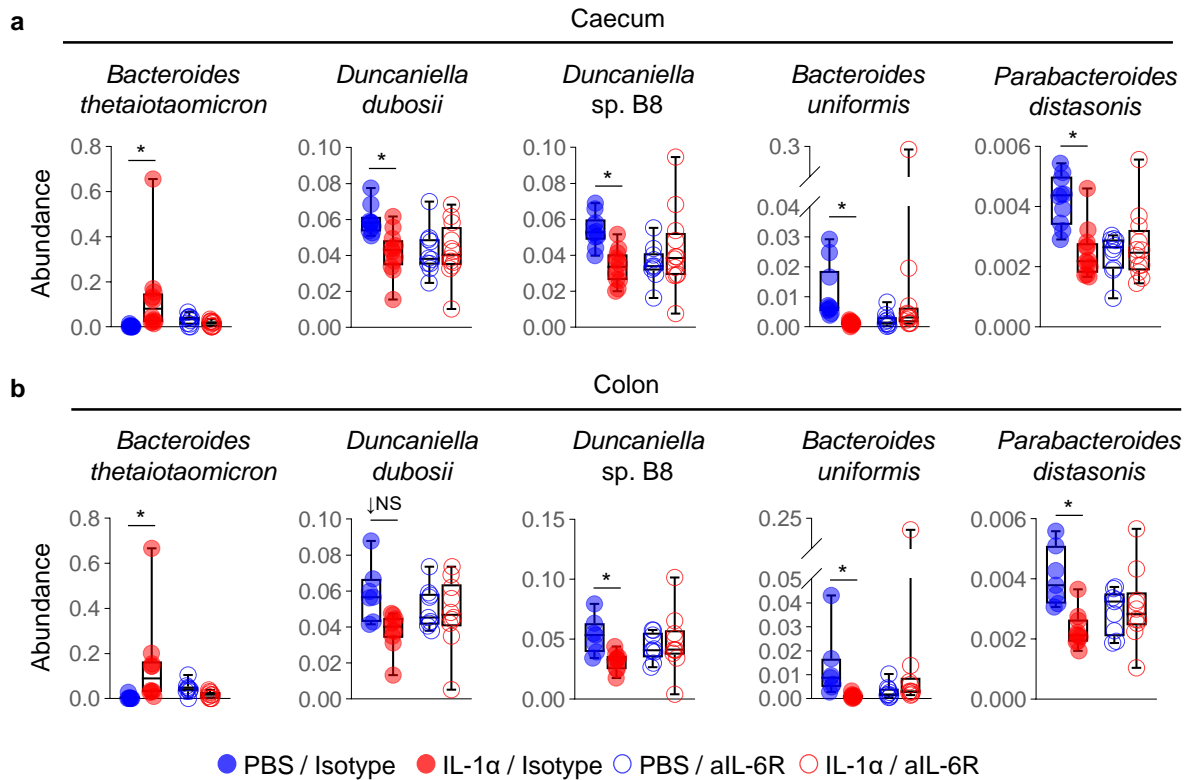


Fig. S4. Blockade of IL-6R modifies the abundance of specific bacterial taxa in the neonatal caecum and colon. Alterations in the abundance of specific bacterial taxa in the neonatal **(a)** caecum and **(b)** colon from the four experimental groups ($n = 10-12$ per group). P-values were determined using two-sided Mann-Whitney U-tests with Holm's correction for multiple comparisons. Data are shown as box-and-whisker plots where midlines indicate medians, boxes indicate interquartile ranges, and whiskers indicate minimum and maximum values. * $p < 0.05$; ↓NS: non-significant tendency for reduction.

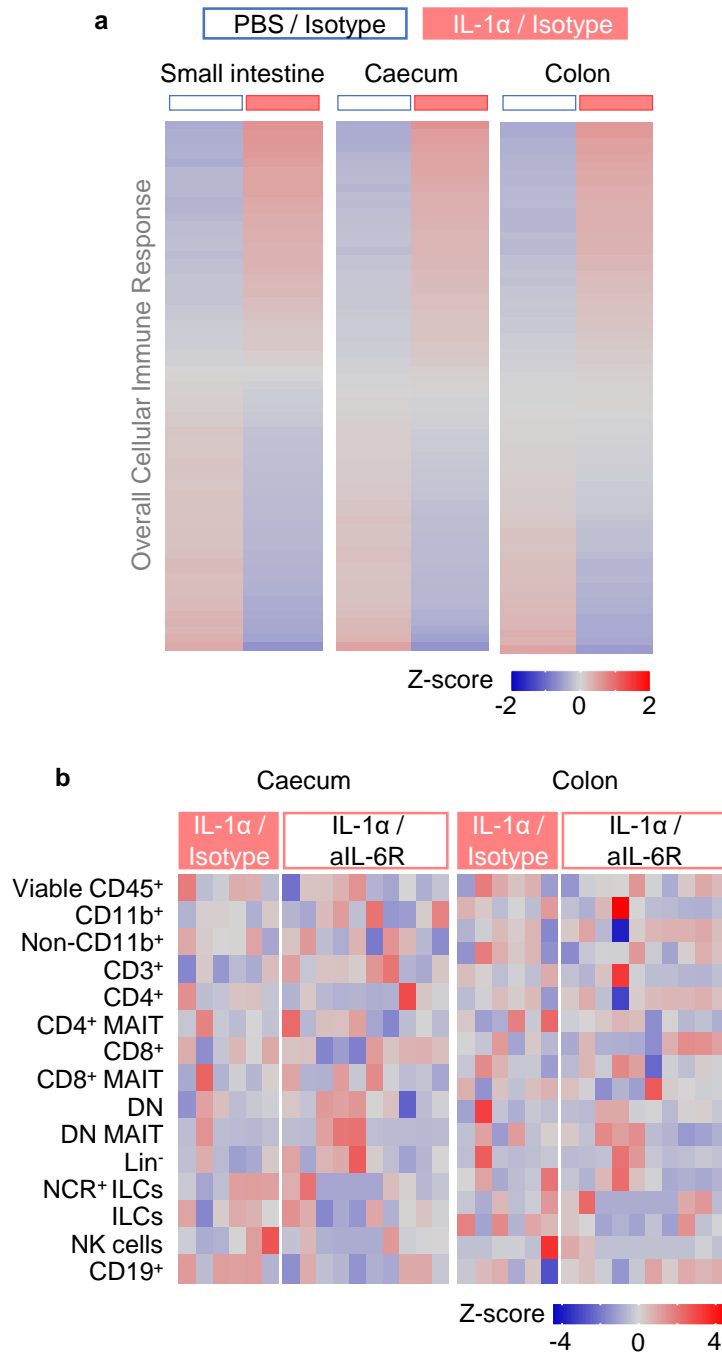


Fig. S5. Leukocyte proportions in the neonatal gut after intra-amniotic IL-1 α exposure or treatment with aIL-6R. (a) Heatmap representation showing Z-scores for proportions of all leukocyte subpopulations analyzed in the small intestine, caecum, and colon of neonates born to dams exposed to intra-amniotic injection of PBS or IL-1 α (n = 5-8 per group). (b) Heatmap representation showing Z-scores for cell proportions of the indicated leukocyte subpopulations in caecum and colon samples from neonates born to dams exposed to IL-1 α and treated with aIL-6R or isotype (n = 5-11 per group). Red indicates increased frequency and blue indicates decreased frequency.

Table S1. TaqMan assays utilised for RT-PCR

Name	Symbol	Assay ID
Actin, beta	<i>Actb</i>	Mm04394036_g1
Glucuronidase, beta	<i>Gusb</i>	Mm01197698_m
Glyceraldehyde-3-phosphate dehydrogenase	<i>Gapdh</i>	Mm99999915_g1
Heat shock protein 90 alpha (cytosolic), class B member 1	<i>Hsp90ab1</i>	Mm00833431_g1
Matrix metalloproteinase 9	<i>Mmp9</i>	Mm00442991_m1
Claudin 4	<i>Cldn4</i>	Mm00515514_s1
Hyaluronan synthase 2	<i>Has2</i>	Mm00515089_m1
Interleukin 1 alpha	<i>Il1a</i>	Mm00439620_m1
Interleukin 1 beta	<i>Il1b</i>	Mm00434228_m1
Interleukin 6	<i>Il6</i>	Mm00446190_m1
Interleukin 10	<i>Il10</i>	Mm01288386_m1
Interleukin 12a	<i>Il12a</i>	Mm00434169_m1
Interleukin 12b	<i>Il12b</i>	Mm01288989_m1
Interleukin 13	<i>Il13</i>	Mm00434204_m1
Interleukin 33	<i>Il33</i>	Mm00505403_m1
Tumor necrosis factor	<i>Tnf</i>	Mm00443258_m1
Interferon gamma	<i>Ifng</i>	Mm01168134_m1
Chemokine (C-C motif) ligand 2	<i>Ccl2</i>	Mm00441242_m1
Chemokine (C-C motif) ligand 3	<i>Ccl3</i>	Mm00441259_g1
Chemokine (C-C motif) ligand 5	<i>Ccl5</i>	Mm01302427_m1
Chemokine (C-C motif) ligand 17	<i>Ccl17</i>	Mm01244826_g1
Chemokine (C-X-C motif) ligand 1	<i>Cxcl1</i>	Mm04207460_m1
Chemokine (C-X-C motif) ligand 9	<i>Cxcl9</i>	Mm00434946_m1
Chemokine (C-X-C motif) ligand 10	<i>Cxcl10</i>	Mm00445235_m1
Chemokine (C-C motif) receptor 5	<i>Ccr5</i>	Mm01963251_s1
CD68 antigen	<i>Cd68</i>	Mm03047343_m1
Interleukin 1 receptor, type I	<i>Il1r1</i>	Mm00434237_m1
Interleukin 10 receptor, alpha	<i>Il10ra</i>	Mm00434151_m1
Interleukin 10 receptor, beta	<i>Il10rb</i>	Mm00434157_m1
Tumor necrosis factor receptor superfamily, member 1a	<i>Tnfrsf1a</i>	Mm00441883_g1
Tumor necrosis factor receptor superfamily, member 1b	<i>Tnfrsf1b</i>	Mm00441889_m1
Purinergic receptor P2X, ligand-gated ion channel, 7	<i>P2rx7</i>	Mm01199500_m1
PYD and CARD domain containing	<i>Pycard</i>	Mm00445747_g1
Nuclear factor of kappa light polypeptide gene enhancer in B cells 1	<i>Nfkb1</i>	Mm00476361_m1
Nuclear factor of kappa light polypeptide gene enhancer in B cells 2	<i>Nfkb2</i>	Mm00479807_m1
NLR family, pyrin domain containing 3	<i>Nlrp3</i>	Mm00840904_m1
NLR family, pyrin domain containing 6	<i>Nlrp6</i>	Mm00460229_m1
Caspase 1	<i>Casp1</i>	Mm00438023_m1
Caspase 4, apoptosis-related cysteine peptidase	<i>Casp11</i>	Mm00432304_m1
Myeloid differentiation primary response gene 88	<i>Myd88</i>	Mm00440338_m1
Arginase, liver	<i>Arg1</i>	Mm00475988_m1
Nitric oxide synthase 2, inducible	<i>Nos2</i>	Mm00440502_m1
Leucine-rich alpha-2-glycoprotein 1	<i>Lrg1</i>	Mm01278767_m1
Absent in melanoma 2	<i>Aim2</i>	Mm01295719_m1
Insulin-like growth factor 2	<i>Igf2</i>	Mm00439564_m1
S100 calcium binding protein A9 (calgranulin B)	<i>S100a9</i>	Mm00656925_m1
Jun proto-oncogene	<i>Jun</i>	Mm07296811_s1
FBJ osteosarcoma oncogene	<i>Fos</i>	Mm00487425_m1
Suppressor of cytokine signaling 3	<i>Socs3</i>	Mm00545913_s1
Toll-like receptor 9	<i>Tlr9</i>	Mm00446193_m1
Glutamate receptor, metabotropic 5	<i>mGluR5</i>	Mm00690332_m1
Regulator of G-protein signaling 4	<i>Rgs4</i>	Mm00501389_m1
KDM1 lysine (K)-specific demethylase 6B	<i>Kdm6b</i>	Mm01332680_m1

Table S2. List of antibodies utilised for flow cytometry.

Antigen/isotype	Fluorochrome	Clone	Company	Cat #	RRID
CD45	AF700	30-F11	BD Biosciences	560510	AB_1645208
CD3	BV650	145-2C11	BD Biosciences	564378	AB_2738779
CD4	PE-Cy5	RM4-5	BD Biosciences	553050	AB_394586
CD8	APC-Cy7	53-6.7	BD Biosciences	557654	AB_396769
CD11b	PE-CF594	M1/70	BD Biosciences	562317	AB_11154422
ID2	APC	ILCID2	ThermoFisher	17-9475-82	AB_2735051
NK1.1	PerCP-Cy5.5	S17016D	Biolegend	156526	AB_2894655
GATA3	BV395	L50-823	BD Biosciences	565448	AB_2739241
ROR γ t	BV421	Q31-378	BD Biosciences	562894	AB_2687545
IFN γ	BV737	XMG1.2	BD Biosciences	564693	AB_2722494
TCR Vb6	PE	RR4-7	Biolegend	140004	AB_10643583
IL10	BV605	JES5-16E3	BD Biosciences	564082	AB_2738582
CD19	BV711	ID3	BD Biosciences	563157	AB_2738035
TGF β	PE-Cy7	TW7-16B4	eBioscience	25-9821-82	AB_2573554
FoxP3	AF488	MF23	BD Biosciences	560403	AB_1645192
IL17A	BV786	TC11-18H10	BD Biosciences	564171	AB_2738642
Mouse / IgG1, κ	APC	P3.6.2.8.1	ThermoFisher	17-4714-82	AB_763649
Rat IgG1, κ	BUV737	R3-34	BD Biosciences	564690	AB_2869604
Rat IgG2b	BV605	R35-38	BD Biosciences	563145	AB_2869464
Mouse IgG1, κ	PE-Cy7	P3.6.2.8.1	eBioscience	25-4714-80	AB_657914
Rat IgG2b	AF488	A95-1	BD Biosciences	557726	AB_396834
Rat IgG1	BV786	R3-34	BD Biosciences	563847	AB_2869525
Mouse IgG2a	BV421	G155-178	BD Biosciences	562439	AB_11151914
Mouse IgG1	BUV395	X40	BD Biosciences	563547	AB_2869503

Table S3. Preterm labour-associated differential expression of *Il6* in murine uterine and decidual cell types.

Location	Cell type	Base Mean	log ₂ Fold Change	Fold Change	lfcSE	Stat	p-value	adj p-value
Myometrium	17_Endothelial	14.852	6.570	94.982	1.351	4.864	1.15E-06	1.63E-04
Decidua	9_Macrophage	48.093	5.773	54.672	0.907	6.362	2.00E-10	1.68E-08
Myometrium	9_Macrophage	65.042	5.496	45.119	0.999	5.499	3.83E-08	6.03E-07
Myometrium	0_Fibroblast-1	43.804	5.352	40.847	1.063	5.034	4.80E-07	2.26E-05
Decidua	2_Stromal-1	29.162	5.296	39.300	1.403	3.776	1.59E-04	0.017
Decidua	13_Epithelial-5 (Luminal)	6.991	5.292	39.183	1.194	4.431	9.38E-06	6.38E-04
Myometrium	15_SMC-1	2.373	5.220	37.264	1.499	3.481	4.99E-04	0.019
Myometrium	14_Epithelial-6 (Secretory)	2.474	4.799	27.834	1.671	2.872	0.004	0.041
Myometrium	3_Monocyte	146.590	4.240	18.894	0.573	7.394	1.43E-13	1.05E-11
Myometrium	12_Stromal-3	31.586	4.186	18.208	1.248	3.355	7.92E-04	0.011
Myometrium	1_Fibroblast-2	47.682	4.020	16.228	1.010	3.981	6.86E-05	0.002
Decidua	0_Fibroblast-1	19.835	3.572	11.896	0.730	4.894	9.89E-07	7.33E-05
Decidua	4_Stromal-2 (Decidua)	7.552	3.472	11.094	0.943	3.681	2.32E-04	0.049
Decidua	3_Monocyte	150.939	3.300	9.850	0.799	4.133	3.58E-05	5.93E-04
Decidua	12_Stromal-3	29.901	2.073	4.208	0.703	2.950	0.003	0.044
Decidua	1_Fibroblast-2	94.814	1.943	3.845	0.608	3.196	0.001	0.031